

Superconductivity in kagome metal $ThRu_3Si_2$

Yi Liu(刘艺), Jing Li(厉静), Wu-Zhang Yang(杨武璋), Jia-Yi Lu(卢佳依), Bo-Ya Cao(曹博雅), Hua-Xun Li(李华旬), Wan-Li Chai(柴万力), Si-Qi Wu(武思祺), Bai-Zhuo Li(李佰卓), Yun-Lei Sun(孙云蕾), Wen-He Jiao(焦文鹤), Cao Wang(王操), Xiao-Feng Xu(许晓峰), Zhi Ren(任之), and Guang-Han Cao(曹光旱)

Citation: Chin. Phys. B, 2024, 33 (**5**): 057401. DOI: 10.1088/1674-1056/ad1c5e
Journal homepage: http://cpb.iphy.ac.cn; http://iopscience.iop.org/cpb

What follows is a list of articles you may be interested in

Robust T_c in element molybdenum up to 160 GPa

Xinyue Wu(吴新月), Shumin Guo(郭淑敏), Jianning Guo(郭鉴宁), Su Chen(陈诉), Yulong Wang(王煜龙), Kexin Zhang(张可欣), Chengcheng Zhu(朱程程), Chenchen Liu(刘晨晨), Xiaoli Huang(黄晓丽), Defang Duan(段德芳), and Tian Cui(崔田)

Chin. Phys. B, 2024, 33 (**4**): 047406. DOI: 10.1088/1674-1056/ad2a78

Spin-polarized pairing induced by the magnetic field in the Bernal bilayer graphene

Yan Huang(黄妍) and Tao Zhou(周涛)

Chin. Phys. B, 2024, 33 (**4**): 047403. DOI: 10.1088/1674-1056/ad102f

Effects of carrier density and interactions on pairing symmetry in a t_{2g} model

Yun-Xiao Li(李云霄), Wen-Han Xi(西文翰), Zhao-Yang Dong(董召阳), Zi-Jian Yao(姚子健), Shun-Li Yu(于顺利), and Jian-Xin Li(李建新)

Chin. Phys. B, 2024, 33 (**1**): 017404. DOI: 10.1088/1674-1056/ad1094

Multi-band analysis on physical properties of superconducting FeSe films

Jian-Tao Che(车剑韬) and Chen-Xiao Ye(叶晨骁)

Chin. Phys. B, 2023, 32 (**9**): 097401. DOI: 10.1088/1674-1056/acd3e5

Flux pinning evolution in multilayer Pb/Ge/Pb/Ge/Pb superconducting systems

Li-Xin Gao(高礼鑫), Xiao-Ke Zhang(张晓珂), An-Lei Zhang(张安蕾), Qi-Ling Xiao(肖祁陵), Fei Chen(陈飞), and Jun-Yi Ge(葛军饴)

Chin. Phys. B, 2023, 32 (**3**): 037402. DOI: 10.1088/1674-1056/ac89e1

SPECIAL TOPIC — Recent progress on kagome metals and superconductors

Superconductivity in kagome metal $ThRu_3Si_2$

Yi Liu(刘艺)[1,2,†,‡], Jing Li(厉静)[1,†], Wu-Zhang Yang(杨武璋)[3], Jia-Yi Lu(卢佳依)[1], Bo-Ya Cao(曹博雅)[2], Hua-Xun Li(李华旬)[1], Wan-Li Chai(柴万力)[1], Si-Qi Wu(武思祺)[1], Bai-Zhuo Li(李佰卓)[4], Yun-Lei Sun(孙云蕾)[5], Wen-He Jiao(焦文鹤)[2], Cao Wang(王操)[4], Xiao-Feng Xu(许晓峰)[2], Zhi Ren(任之)[3], and Guang-Han Cao(曹光旱)[1,6,7,§]

[1] *School of Physics, Zhejiang University, Hangzhou* 310058, *China*
[2] *Department of Applied Physics, Zhejiang University of Technology, Hangzhou* 310023, *China*
[3] *School of Science, Westlake Institute for Advanced Study, Westlake University, Hangzhou* 310064, *China*
[4] *Department of Physics, Shandong University of Technology, Zibo* 255049, *China*
[5] *School of Information and Electrical Engineering, Zhejiang University City College, Hangzhou* 310015, *China*
[6] *Interdisciplinary Center for Quantum Information, and State Key Laboratory of Silicon and Advanced Semiconductor Materials, Zhejiang University, Hangzhou* 310058, *China*
[7] *Collaborative Innovation Centre of Advanced Microstructures, Nanjing University, Nanjing* 210093, *China*

(Received 22 December 2023; revised manuscript received 5 January 2024; accepted manuscript online 9 January 2024)

We report the physical properties of $ThRu_3Si_2$ featured with distorted Ru kagome lattice. The combined experiments of resistivity, magnetization and specific heat reveal bulk superconductivity with $T_c = 3.8$ K. The specific heat jump and calculated electron–phonon coupling indicate a moderate coupled BCS superconductor. In comparison with $LaRu_3Si_2$, the calculated electronic structure in $ThRu_3Si_2$ shows an electron-doping effect with electron filling lifted from 100 meV below flat bands to 300 meV above it. This explains the lower superconducting transition temperature and weaker electron correlations observed in $ThRu_3Si_2$. Our work suggests the T_c and electronic correlations in the kagome superconductor could have an intimate connection with the flat bands.

Keywords: superconductivity, kagome lattice, flat band

PACS: 74.70.–b, 74.25.–q, 74.25.Ha **DOI:** 10.1088/1674-1056/ad1c5e

1. Introduction

Recently, compounds with kagome lattice have attracted lots of attentions for the unique electronic structure and magnetic frustration,[1,2] which provides an exciting platform to study rich quantum physics, such as quantum spin liquid,[3–6] nontrivial band topology[7–9] and superconductivity (SC).[10–16] One of the most exotic features in the electronic structure of the kagome lattice is the flat band with little dispersion in k space, which results from the destructive interference of electron wave functions. The localization of electrons near the Fermi level (E_F) on the flat band is expected to bring high density of electronic states and possible strong electronic correlation.[17,18] For superconductivity with conventional phonon-mediated pairing, larger density of states (DOS) usually results in higher critical temperature, while for the case of unconventional non-phonon-mediated paring, the enhanced electron–electron correlation is also prone to yield high-temperature SC. Therefore, it is promising to access flat bands in specialized system to realize higher critical temperature or even unconventional SC.

Recently, new kagome lattice compound $CsCr_3Sb_5$, with flat bands closely above the Fermi level, presents moderate electronic correlations and unconventional SC under pressure of ~ 4 GPa.[19] The mechanism of its unconventional SC and the effect of flat bands are still unclear. Another traditional family of kagome metal with SC and flat bands close to the Fermi level is intermetallic 132 RT_3X_2 phases, where R and T represent a rare-earth element and a transition metal respectively, and X stands for Si or B. RT_3X_2 crystalizes in hexagonal layered $CeCo_3B_2$ structure, with transition metal T being organized in a distorted kagome layer. Superconductivity is discovered in many materials of RT_3X_2 family, such as $ThRu_3B_2$, $LaRh_3B_2$, $LuOs_3B_2$, $LaIr_3B_2$, $ThIr_3B_2$,[20] YRu_3Si_2, $LaRu_3Si_2$, $ThRu_3Si_2$,[21] $CeRu_3Si_2$[22,23] and $LaIr_3Ga_2$.[24] Recently, $LaRu_3Si_2$ with the highest T_c in RT_3X_2 family, attracted much attention for the interesting electronic structure with flat band close to the E_F and associated strong correlation.[25–27] As revealed by the DFT calculation, the flat band is 100 meV above the E_F. Thus, it is possible to tune the flat bands to the Fermi level by introducing extra electrons to achieve a maximum impact on superconductivity and electron correlations.[26] The structure and superconductivity of $ThRu_3Si_2$ have been reported 30 years ago,[21,28] but the physical properties of normal state and superconductivity have not been systematically investigated yet. Compared with La, Th has similar ion radius, but tends to con-

[†]These authors contributed equally to this work.
[‡]Corresponding author. E-mail: liuyiphy@zjut.edu.cn
[§]Corresponding author. E-mail: ghcao@zju.edu.cn

© 2024 Chinese Physical Society and IOP Publishing Ltd

tribute one more electron. Hence, it's necessary to give a detailed research on this kagome superconductor.

In this work, we carry out a detailed investigation on the superconductivity and normal state of $ThRu_3Si_2$. The measurements of resistivity, magnetism and specific heat demonstrate bulk SC below 3.8 K. Our experimental results suggest a moderate coupled BCS superconductor with electron correlations. Besides, compared with $LaRu_3Si_2$, the calculated band structure using first-principles density functional-theory (DFT) shows electron-doping effect, with the Fermi level shifting from below the flat band to above it.

2. Experimental methods

$ThRu_3Si_2$ polycrystal was synthesized through arc melting. Firstly, the high-purity thorium metal was extracted from thorium oxide as previously reported.[29] The prepared Th button was scraped into powder and then mixed with Ru (99.9%) and Si (99.9%) powder. To avoid the formation of $ThRu_2Si_2$, 15% extra Ru powder was added. The mixture was ground thoroughly and pressed into a pellet, which was then welded in an arc furnace with the current of 45 A. The process was repeated twice to achieve the uniformity. The compositions of the as-prepared sample were measured by energy-dispersive x-ray spectroscopy (EDS) on a scanning electron microscope (Hitachi S-3700N) equipped with an Oxford Instruments XMax spectrometer, and the determined molar ratio is Th:Ru:Si = 1:3:2.1. X-ray diffraction (XRD) was carried out on a PANalytical x-ray diffractometer (Model EMPYREAN) with a monochromatic Cu-$K_{\alpha 1}$ radiation at room temperature. The diffraction peaks were indexed by $ThRu_3Si_2$ and Ru phases, with the percentage of Ru below 10% concluded from the intensity ratio of the maximum peaks. As shown in Fig. 1, the main diffraction peaks can be indexed by the $P6_3/m$ space group (No. 176) with $a = 5.613(2)$ Å and $c = 7.190(1)$ Å, which is consistent with the previous report.[28] Electrical resistivity was measured with four-electrode technique on a brick-shaped polycrystal, while the heat capacity measurement employed the thermal relaxation method with a quantum design physical property measurement system (PPMS-9). The magnetization measurements were performed on the SQUID-VSM magnetometer (MPMS-5).

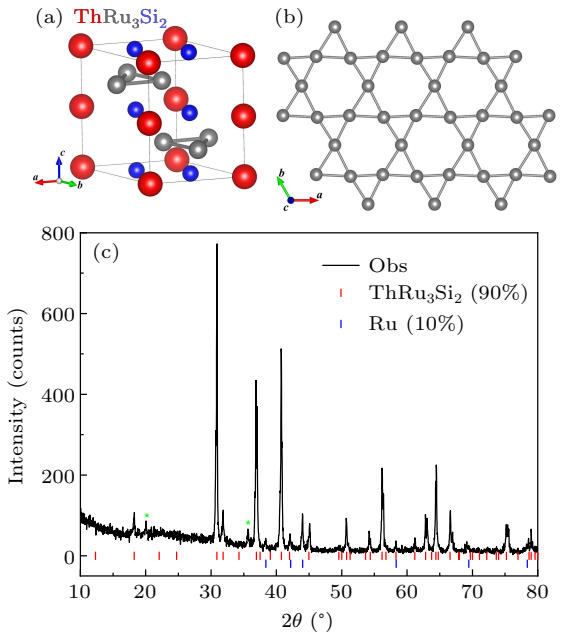


Fig. 1. (a) Crystal structure of $ThRu_2Si_2$, which is formed by the stack of Th (red), Si (blue) and Ru (grey) layers along c axis. (b) Top view of the distorted kagome lattice of Ru atoms. (c) Powder x-ray-diffraction pattern of $ThRu_3Si_2$ sample. The molar ratio of $ThRu_3Si_2$ and the impurity phase of Ru is about 9:1. There are two unidentified small peaks labelled with $*$.

3. Results

The resistivity shows metallic behavior with a large hump below 300 K as present in Fig. 2(a), which is similar to the other RT_3X_2 compounds.[23–25,30] The absolute resistivity at room-temperature is about 68 μΩ·cm and the residual resistivity ratio RRR $= \rho_{300\ \mathrm{K}}/\rho_{4\ \mathrm{K}}$ reaches 7. Note that, the resistivity and RRR are mainly affected by the grain boundary effect in polycrystal instead of their intrinsic conductivity. Superconductivity is observed at low temperature with onset at 3.9 K and zero point at 3.7 K. We define the superconducting transition temperature, $T_c = 3.8$ K, which corresponds to the middle point where the resistivity is half of that in normal state. Under external fields, the transition is suppressed to lower temperatures and the temperature dependence of the upper-critical field $\mu_0 H_{c2}(T)$ is shown in Fig. 2(c). The $\mu_0 H_{c2}(T)$ can be well fitted by two-band model.[31] The fitted parameters of diffusivity ratio η, intra-band scattering λ_1, λ_2 and inter-band scattering $\lambda_{12} = \lambda_{21}$ of the two bands are 25.27(4), 0.80(1), 0.12(2) and 0.28(1) respectively. The upper-critical field at zero temperature $H_{c2}(0)$ is 1.45 T, which is far below the Pauli limit $\mu_0 H_{c2}^{\mathrm{P}} = 1.84 T_c = 6.95$ T, suggesting the orbital pairing-broken mechanism is prominent in $ThRu_3Si_2$. We also measure the magnetoresistance up to 9 T at selected temperatures, as shown in Fig. 2(d). The magnetoresistance is about 13% at 5 K and 9 T.

The temperature dependence of magnetic susceptibility is measured in zero-field cooling (ZFC) and field-cooling (FC) modes as shown in Fig. 3(a). The diamagnetism appears at about 3.7 K, which corresponds to the zero point in resistivity. The superconducting volume fraction approaches above $\sim 90\%$ at 1.8 K in ZFC mode, indicating bulk SC here. The Meissner screening in FC mode decreases to only about half of that in ZFC mode. The weaker diamagnetic signal in FC mode indicates flux pinning in a type Ⅱ superconductor. Figure 3(c) shows the magnetization curves at different temperatures below SC. The lower critical fields H_{c1} are determined from the fields where the magnetization $4\pi M$ starts to deviate from linearity. The temperature dependence of H_{c1} is fitted by the Ginzburg–Landau formula $H_{c1} = H_{c1}(0)[(1-(T/T_c)^2)]$. The $H_{c1}(0)$, lower critical field at 0 K, is about 89.9(1) Oe.

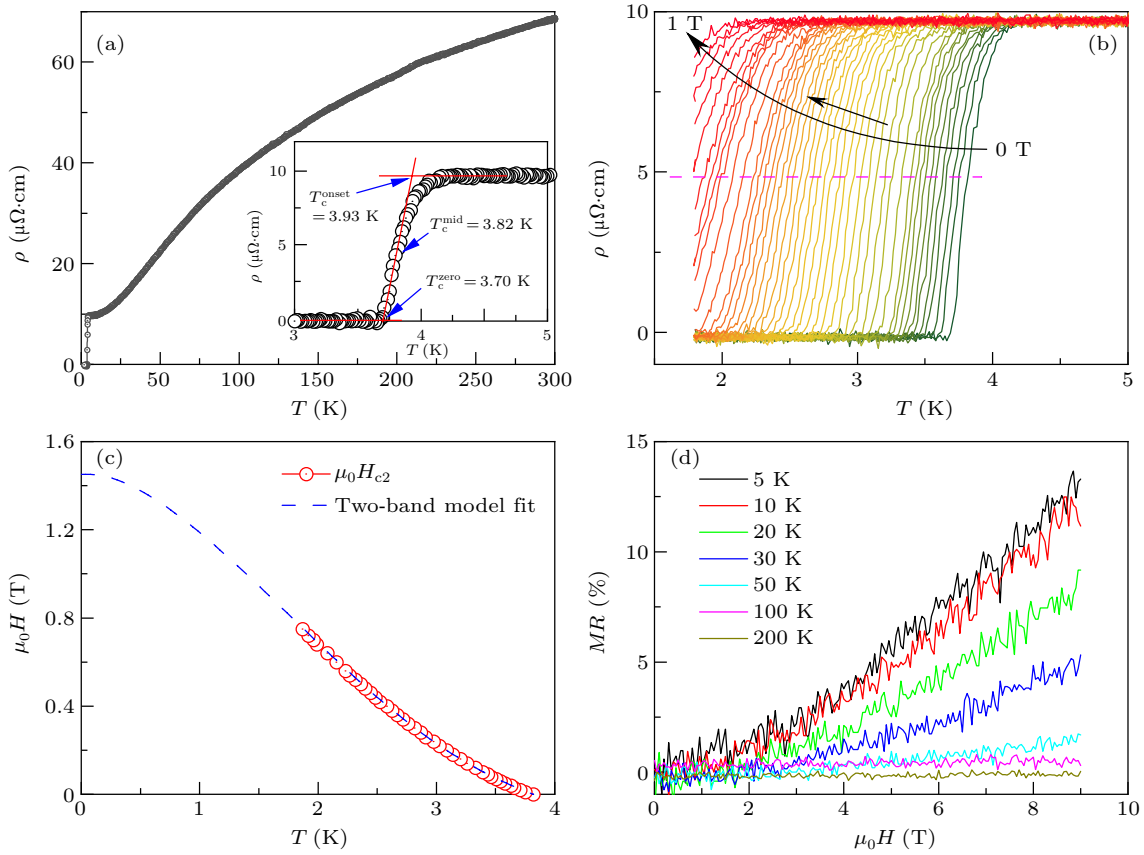


Fig. 2. (a) Temperature dependence of resistivity for $ThRu_3Si_2$. The inset shows the definitions of the onset, middle and zero points of the resistivity drop. (b) Resistivity transition from 1.8 K to 5 K under different magnetic fields from 0 to 1 T. The horizontal dashed pink line is located at half of the normal resistivity to determine the superconducting transition temperatures under fields. (c) Temperature dependence of the upper critical field $\mu_0 H_{c2}(T)$. The dashed blue line is the fit of the two-band model in the dirty limit. (d) Magnetoresistance is measured at selected temperatures.

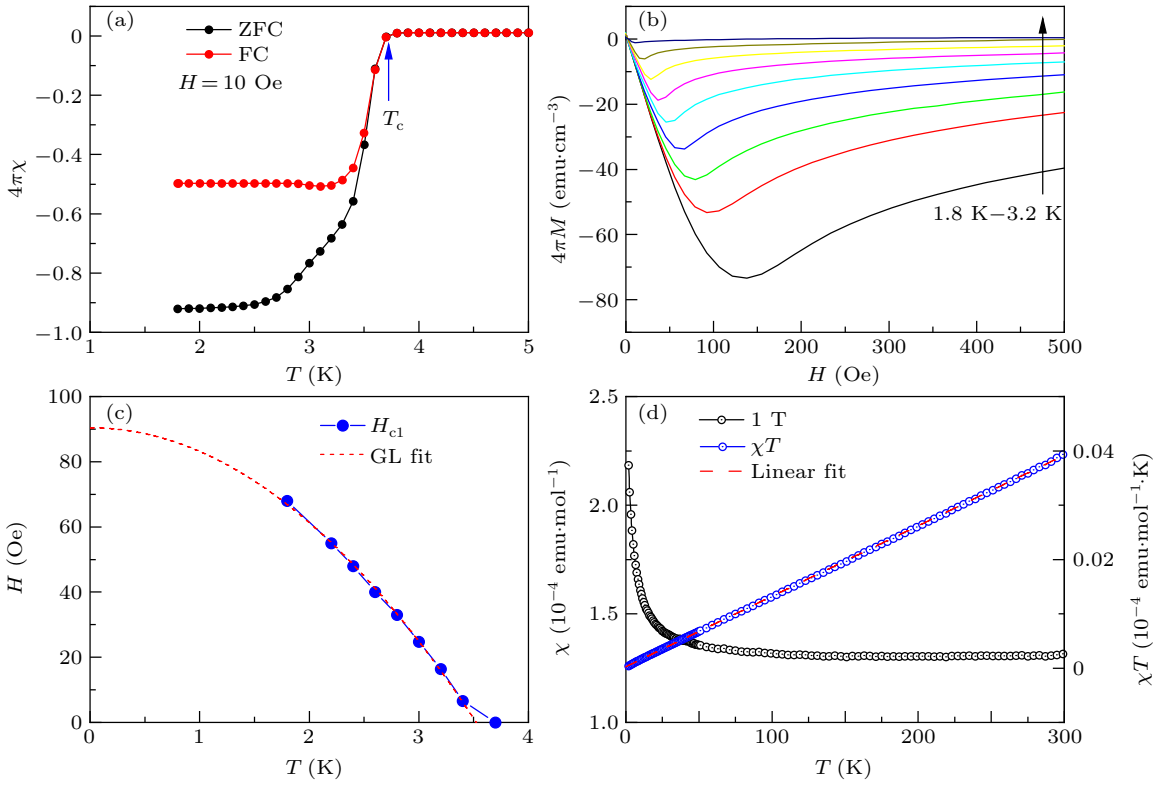


Fig. 3. (a) The low-temperature susceptibility for $ThRu_3Si_2$ in ZFC (black) and FC (red) modes under a magnetic field of 10 Oe. (b) Field dependence of initial magnetization at various temperatures below T_c. (c) Temperature dependence of the lower critical field $H_{c1}(T)$. (d) Temperature dependence of magnetic susceptibility χ at 1 T. The right axis corresponds to χT, and the dashed red line is linear fit of χT.

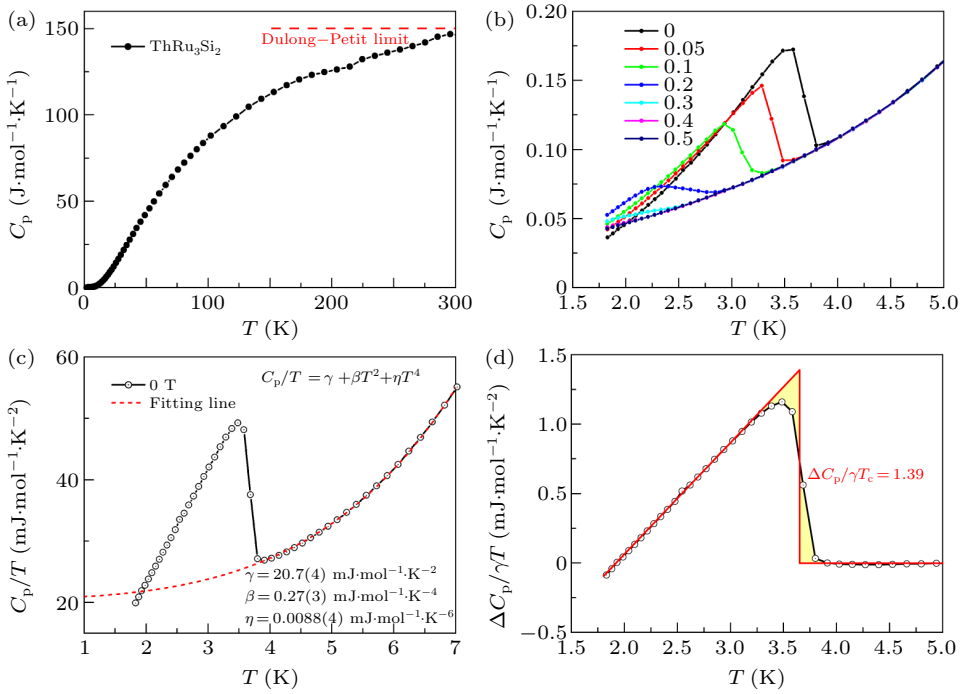


Fig. 4. (a) Temperature dependence of specific heat C_p for $ThRu_3Si_2$. (b) Low-temperature C_p under various fields. (c) Plot of C_p/T versus T below 7 K. The dashed red line is the fit based on the formula $C_p/T = \gamma + \beta T^2 + \eta T^4$. (d) The specific-heat contribution from SC by subtracting the electrons' and phonons' parts.

The susceptibility under the field of 1 T is nearly independent of temperature above 150 K, and the tail at low temperature is possibly induced by tiny paramagnetic impurities or defects, as present in Fig. 3(d). To simplify, we consider the susceptibility to be described by $\chi = \chi_0 + C/T$, where the term of C/T is the contribution from the paramagnetic impurities or defects and the χ_0 is a temperature-independent term. As shown in the right side of Fig. 3(d), the linear fitting of χT versus T yields $\chi_0 = 1.30(4) \times 10^{-4}$ emu/mol and $C = 2.65(7) \times 10^{-4}$ emu/(mol·K). The constant C corresponds to a small effective moment of 0.05 μ_B/f.u., demonstrating the extrinsic paramagnetism. The χ_0 is considered to be contributed by several terms, $\chi_0 = \chi_P + \chi_{core} + \chi_{VV} + \chi_L$, where χ_P is the Pauli susceptibility and the other three terms corresponding to diamagnetic atomic-core susceptibility, the van Vleck paramagnetic susceptibility, and the Landau diamagnetic susceptibility, respectively. The χ_{core} is estimated by the Pascal method with the value of 1.18×10^{-4} emu/mol,[32] while the χ_L is about $-1/3\chi_P$. The χ_{VV} usually takes place in rare-earth ions with an even number of electrons in the unfilled 4f shells, thus we ignore the contribution of van Vleck magnetism here. Therefore, the χ_P is estimated to be 3.72×10^{-4} emu/mol.

The temperature dependence of specific heat $C_p(T)$ is present in Fig. 4(a), which saturates at the Dulong–Petit limit of $3NR = 150$ J·K^{-1}·mol^{-1} at room temperature, where the N is the number of atoms per formula unit and R is the gas constant. At low temperature, the contribution from itinerant electrons is remarkable to specific heat. Figure 4(b) shows the fitting of C_p/T below 7 K using the formula $C_p/T = \gamma + \beta T^2 + \eta T^4$, where the γ is Sommerfeld coefficient corresponding to specific heat of electrons, and the two higher order terms are the contribution of phonons.[33] The fitting gives $\gamma = 20.7(4)$ mJ·K^{-2} and Debye temperature $\theta_D = 351(5)$ K. The θ_D is calculated by the formula $\theta_D = (\frac{12\pi^4}{5\beta}NR)^{1/3}$. A jump corresponding to the superconducting transition is observed at 3.8 K, which increases to maximum at 3.6 K, corresponding to a transition width of 0.2 K, which matches the sharp transition in resistivity. The transition shifts to lower temperature under an external magnetic field, and is not observable above 1.8 K at 0.5 T. The specific heat jumps at T_c, $\Delta C/(\gamma T_c) \sim 1.39$, further confirming bulk SC in $ThRu_3Si_2$. This value is very close to 1.43, which is the theoretical value of BCS theory in the weak coupling limit. Based on the Debye temperature, the electron–phonon coupling constant λ_{ep} can be also estimated through McMillan equation[34]

$$\lambda_{ep} = \frac{1.04 + \mu^* \ln(\frac{\theta_D}{1.45T_c})}{(1 - 0.62\mu^*)\ln(\frac{\theta_D}{1.45T_c}) - 1.04}, \quad (1)$$

where the μ^* is the Coulomb pseudopotential parameter with a typical value of 0.13. The λ_{ep} value for $ThRu_3Si_2$ is 0.57, which is close to the values of 0.67 in $LaRu_3Si_2$ ($\theta_D = 412$ K and $T_c = 7.8$ K) and 0.5 in YRu_3Si_2.[30] Therefore, a moderate strength of electron-coupling is expected in the Ru based 132 system.

To get more insights into the properties of $ThRu_3Si_2$, the density of electronic states and electronic band structure are calculated based on the density-functional theory. Figure 5(a) shows the projected band structure of $ThRu_3Si_2$. There are two bands cross the E_F, which is consistent with the two-bands fitting of the upper critical field $\mu_0 H_{c2}(T)$. The bands

from Γ to A show prominent dispersion, indicating the two-dimensional feature is not remarkable in $ThRu_3Si_2$. Additionally, a possible Dirac point with the bands cross of Si 3p and Ru 4d electrons appears about 70 meV above E_F, as shown in the circled area. The projected density of state (DOS) shown in Fig. 5(a) demonstrates the states around E_F are mainly contributed by the Ru 4d electrons. The total DOS N_E at E_F is 4.06 $eV^{-1}\cdot f.u.^{-1}$. This value is about one third of 11.78 $eV^{-1}\cdot f.u.^{-1}$ inferred from Pauli susceptibility with the formula: $\chi_P = \mu_B^2 N_E$, and also less than half of 8.7 $eV^{-1}\cdot f.u.^{-1}$ obtained from Sommerfeld coefficient through the formula $\gamma = \frac{1}{3}\pi^2 k_B^2 N_E$, indicating the contribution of quasiparticle interactions in itinerant electrons. Wilson ratio is usually used to estimate the electron correlation effect, which is calculated with the equation $R_W = \frac{1}{3}(\frac{\pi k_B}{\mu_B})^2 \frac{\chi_P}{\gamma}$. The obtained R_W is 1.31, slightly larger than 1, indicating the existence of correlation of quasi-particles.

Figure 5(d) shows the band structure around E_F. A Dirac point at the K point with linear dispersion is observed at 700 meV below the E_F. And the van Hove point is also found away from E_F (300 meV) at M point. Besides, the flat bands, which are common in two-dimensional kagome lattice from Γ to M point as shown in Fig. 5(c), present severe dispersion. Compared with the results of $LaRu_3Si_2$, despite of the slight difference in the details of the energy bands, the E_F is basically lifted up about 400 meV in $ThRu_3Si_2$, which can be considered as electron doping. The flat bands are farther away from the E_F in $ThRu_3Si_2$ (300 meV above E_F) than that in $LaRu_3Si_2$ (100 meV below E_F).

For comparison, we list the physical parameters of $LaRu_3Si_2$ and $ThRu_3Si_2$ in Table 1. There are no many differences in the cell parameters a and c, which can be ascribed to the similar ion radius of La^{3+} and Th^{4+}. However, the critical temperature of superconductivity is doubled in $LaRu_3Si_2$, which should mainly originate from the significant contrast in the density of states near the Fermi level, as revealed in the DFT calculations. The Fermi level is further away from the flat bands. Additionally, the stronger electron–phonon coupling, which is proportional to the Debye temperature, also contributes higher T_c in $LaRu_3Si_2$. Similar to $LaRu_3Si_2$,[25–27,35] $ThRu_3Si_2$ is also considered to be a moderately coupled BCS superconductor according to the values of λ_{ep}. The specific heat jump at T_c in the two compounds is close to the theoretical value of 1.43. In $ThRu_3Si_2$, the upper critical field $\mu_0 H_{c2}(T)$ can be well fitted by a two band model, which is also consistent with the multi-band feature shown in the DFT calculation.

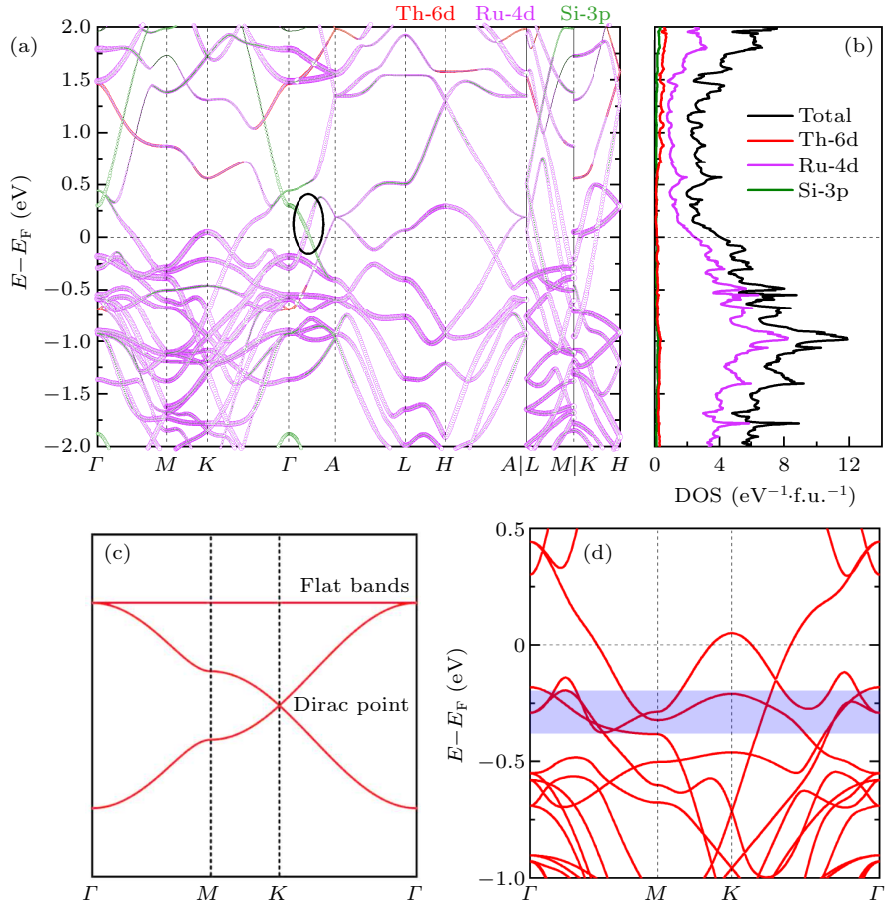


Fig. 5. (a) and (b) DFT calculation of band structure and projected density of states without spin-orbital coupling. The black circle shows the possible Dirac point near the Fermi level. (c) Typical band structure of kagome lattice with Dirac cone at the K point and a flat band across the Brillouin zone. (d) The band structure near E_F. The blue region highlights the kagome flat band.

Table 1. Physical property parameters of $LaRu_3Si_2$ and $ThRu_3Si_2$.

Parameters	$LaRu_3Si_2$[25]	$ThRu_3Si_2$
a (Å)	5.68	5.614
c (Å)	7.13	7.191
T_c (K)	7.8	3.8
RRR	5	7
χ_P (10^{-4} emu·mol^{-1}·Oe^{-1})	14.4	3.72
γ (mJ·K^{-2}·mol^{-1})	36.8	20.7
θ_D (K)	412	351
λ_{ep}	0.67	0.57
$\Delta C/\gamma T_c$	1.36	1.39
R_W	2.88	1.31
N_E (eV^{-1}·f.u.$^{-1}$)	~ 7	4.06

Interestingly, the total DOS at E_F estimated from the specific-heat coefficient γ and Pauli paramagnetism χ_P, are much larger than that obtained by DFT calculation, suggesting an electron-mass renormalization due to correlation effect. This renormalization is more prominent in $LaRu_3Si_2$. On the other hand, the Wilson ratio R_W, which is equal to 1 for noninteracting free electron gas system, are 2.88 and 1.31 for $LaRu_3Si_2$ and $ThRu_3Si_2$ respectively, also suggesting the existence of electron correlations and it is stronger in $LaRu_3Si_2$. The correlation effect is considered to arise from the flat bands. We note that the Fermi level is shifted from 100 meV below flat bands in $LaRu_3Si_2$ to 300 meV above it in $ThRu_3Si_2$. The effect of flat bands is weakened as it is away from the Fermi level, accompanied by the decrease of density of states and suppression of electron correlations.

4. Conclusion

In summary, the bulk superconductivity of kagome metal $ThRu_3Si_2$ with $T_c = 3.8$ K is investigated through resistivity, magnetism and specific heat measurements. The temperature dependence of the upper critical field suggests two superconducting gaps in $ThRu_3Si_2$ with $H_{c2}(0) = 1.45$ T, which is well below the Pauli limit. The specific heat jump and calculated electron–phonon coupling indicate a moderately electron–phonon coupled superconductor. On the other hand, affected by the flat bands, the electron correlation in $ThRu_3Si_2$ is relatively weakened compared with $LaRu_3Si_2$. Since the Fermi level in $ThRu_3Si_2$ shifts up about 400 meV arising from the introduction of extra electrons by substituting La with Th, the flat bands are further away from the Fermi level, which explains the reduction of DOS and electron correlations. Therefore, it is expectable that higher T_c and stronger electron correlations may appear in Th slightly doped $LaRu_3Si_2$ with flat bands right on the Fermi level.

Acknowledgments

Project supported by the National Natural Science Foundation of China (Grant Nos. 12050003, 12004337, and 12274369) and the Zhejiang Provincial Natural Science Foundation of China (Grant No. LQ21A040011).

References

[1] Yin J X, Lian B and Hasan M Z 2022 *Nature* **612** 647
[2] Chowdhury N, Khan K I A, Bangar H, Gupta P, Yadav R S, Agarwal R, Kumar A and Muduli P K 2023 *Proceedings of The National Academy of Sciences India Section A-Physical Sciences* **93** 477
[3] Han T H, Helton J S, Chu S, Nocera D G, Rodriguez-Rivera J A, Broholm C and Lee Y S 2012 *Nature* **492** 406
[4] Yan S, Huse D A and White S R 2011 *Science* **332** 1173
[5] Balents L 2010 *Nature* **464** 199
[6] Olariu A, Mendels P, Bert F, Duc F, Trombe J C, de Vries M A and Harrison A 2008 *Phys. Rev. Lett.* **100** 087202
[7] Xue H, Yang Y, Gao F, Chong Y and Zhang B 2019 *Nat. Mater.* **18** 108
[8] Liu E, Sun Y, Kumar N, Muechler L, Sun A, Jiao L, Yang S Y, Liu D, Liang A, Xu Q, Kroder J, Suess V, Borrmann H, Shekhar C, Wang Z, Xi C, Wang W, Schnelle W, Wirth S, Chen Y, Goennenwein S T B and Felser C 2018 *Nat. Phys.* **14** 1125
[9] Ye L, Kang M, Liu J, von Cube F, Wicker C R, Suzuki T, Jozwiak C, Bostwick A, Rotenberg E, Bell D C, Fu L, Comin R and Checkelsky J G 2018 *Nature* **555** 638
[10] Peng C, Jiang Y F, Sheng D N and Jiang H C 2021 *Adv. Quantum Technol.* **4** 2000126
[11] Wang Q, Qiu X L, Pei C, Gong B C, Gao L, Zhao Y, Cao W, Li C, Zhu S, Zhang M, Chen Y, Liu K and Qi Y 2023 *New J. Phys.* **25** 043001
[12] Jiang K, Wu T, Yin J X, Wang Z, Hasan M Z, Wilson S D, Chen X and Hu J 2023 *Natl. Sci. Rev.* **10** nwac199
[13] Chen H, Hu B, Ye Y, Yang H and Gao H J 2022 *Chin. Phys. B* **31** 097405
[14] Ortiz B R, Sarte P M, Kenney E M, Graf M J, Teicher S M L, Seshadri R and Wilson S D 2021 *Phys. Rev. Mater.* **5** 034801
[15] Ortiz B R, Teicher S M L, Hu Y, Zuo J L, Sarte P M, Schueller E C, Abeykoon A M M, Krogstad M J, Rosenkranz S, Osborn R, Seshadri R, Balents L, He J and Wilson S D 2020 *Phys. Rev. Lett.* **125** 247002
[16] Ni S, Ma S, Zhang Y, Yuan J, Yang H, Lu Z, Wang N, Sun J, Zhao Z, Li D, Liu S, Zhang H, Chen H, Jin K, Cheng J, Yu L, Zhou F, Dong X, Hu J, Gao H J and Zhao Z 2021 *Chin. Phys. Lett.* **38** 057403
[17] Bilitewski T and Moessner R 2018 *Phys. Rev. B* **98** 235109
[18] Bergman D L, Wu C and Balents L 2008 *Phys. Rev. B* **78** 125104
[19] Liu Y, Liu Z Y, Bao J K, Yang P T, Ji L W, Liu J Y, Xu C C, Yang W Z, Chai W L, Lu J Y, Liu C C, Wang B S, Jiang H, Tao Q, Ren Z, Xu X F, Cao C, Xu Z A, Cheng J G and Cao G H 2023 arXiv:2309.13514 [cond-mat.supr-con]
[20] Ku H, Meisner G, Acker F and Johnston D 1980 *Solid State Commun.* **35** 91
[21] Barz H 1980 *Mater. Res. Bull.* **15** 1489
[22] Godart C, Gupta L, Parks R, Rauschwalbe U, Alheim U, Gottwick U, Lieke W and Steglich F 1984 *Ann. Chim.-Sci. Mat.* **9** 979
[23] Rauchschwalbe U, Lieke W, Steglich F, Godart C, Gupta L and Parks R 1984 *Phys. Rev. B* **30** 444
[24] Gui X and Cava R J 2022 *Chem. Mater.* **34** 2824
[25] Li S, Zeng B, Wan X, Tao J, Han F, Yang H, Wang Z and Wen H H 2011 *Phys. Rev. B* **84** 214527
[26] Mielke C, Qin Y, Yin J X, Nakamura H, Das D, Guo K, Khasanov R, Chang J, Wang Z Q, Jia S, Nakatsuji S, Amato A, Luetkens H, Xu G, Hasan M Z and Guguchia Z 2021 *Phys. Rev. Mater.* **5** 034803
[27] Kishimoto Y, Kawasaki Y, Ohno T, Gupta L and Ghosh G 2004 *J. Phys. Soc. Jpn.* **73** 190
[28] Vandenberg J and Barz H 1980 *Mater. Res. Bull.* **15** 1493
[29] Wang C, Wang Z C, Mei Y X, Li Y K, Li L, Tang Z T, Liu Y, Zhang P, Zhai H F, Xu Z A and Cao G H 2016 *J. Am. Chem. Soc.* **138** 2170
[30] Gong C, Tian S, Tu Z, Yin Q, Fu Y, Luo R and Lei H 2022 *Chin. Phys. Lett.* **39**
[31] Gurevich A 2003 *Phys. Rev. B* **67** 184515
[32] Bain G A and Berry J F 2008 *J. Chem. Educ.* **85** 532
[33] Yang H and Lin J 2001 *J. Phys. Chem. Solids* **62** 1861
[34] Mcmillan W 1968 *Phys. Rev.* **167** 331
[35] Li B, Li S and Wen H H 2016 *Phys. Rev. B* **94** 094523